

FORMATION OF Ti_3Al AND ITS EMBRITTLING EFFECTS
ON TITANIUM-ALUMINUM ALLOYS

by

Frank Edward Brauer

Thesis submitted to the Graduate Faculty of the
Virginia Polytechnic Institute
in candidacy for the degree of
MASTER OF SCIENCE
in
Metallurgical Engineering

APPROVED:

Chairman, Roy C. Wilcox

C.R. Houska

J.L. Lytton

T.P. Floridis

May, 1967
Blacksburg, Virginia

TABLE OF CONTENTS

	Page
I. INTRODUCTION	6
II. LITERATURE REVIEW	7
A. Titanium-Aluminum Diagram	7
B. Ti_3Al	8
C. Ordering and Embrittlement	9
III. EXPERIMENTAL PROCEDURE	11
A. Material	11
B. Heat Treatment	11
C. Metallography	12
D. Stress Corrosion and Charpy V-notch	12
Impact Tests	
IV. RESULTS AND DISCUSSION	14
A. Metallography	14
B. Stress Corrosion and Charpy V-notch	16
Impact Tests	
V. CONCLUSIONS	19
VI. FUTURE WORK	21
VII. BIBLIOGRAPHY	22
VIII. ACKNOWLEDGEMENTS	26
IX. VITA	27

LIST OF TABLES

	Page
TABLE I. Mutual Solid Solubilities of Aluminum and Transition Elements	28
TABLE II. Composition of Titanium Sponge and Aluminum Shot Used to Prepare Alloy Buttons	29
TABLE III. Data on Ti-Al Forgings	30
TABLE IV. Stress Corrosion and Impact Data for 5 Weight Percent Aluminum Alloy	31
TABLE V. Stress Corrosion and Impact Data for 6 Weight Percent Aluminum Alloy	32
Table VI. Stress Corrosion and Impact Data for 7 Weight Percent Aluminum Alloy	33
TABLE VII. Stress Corrosion and Impact Data for 8 Weight Percent Aluminum Alloy	34

LIST OF FIGURES

	Page
Figure 1. Comparison of Proposed Ti-Al Diagrams.	35
Figure 2. Titanium-Rich End of the Ti-Al System.	36
Figure 3. DO_{19} Structure of Ti_3Al .	37
Figure 4. Heats of Formation in Ti-Al System.	38
Figure 5. Brown Type Stress Corrosion Apparatus	39
Figure 6. Various Zones that Appear in the Fractured Surface of Titanium Alloys After Exposure to Stress in a Marine Environment in the Presence of a Flaw.	40
Figure 7. Typical As Melted Structure of Alloy Buttons, Ti- 6.5 Weight Percent Aluminum. 50X	41
Figure 8. Typical Hot Forged Structure, Ti-8 Weight Percent Aluminum, Hot Forged in Beta Field. 100X	42
Figure 9. Ti_3Al Visible in Widmanstatten Platelet Boundaries. 50X, 1000X	43
Figure 10. Ti_3Al Annealed Out of Platelet Boundaries. 1000X	44
Figure 11. Martensitic Structure at Prior Platelet Boundaries. 1000X	45
Figure 12. Segregation Anneal of Ti-4.1 Weight Percent Aluminum Alloy. 50X, 1000X	46
Figure 13. Segregation Anneal of Ti-6.5 Weight Percent Aluminum Alloy. 50X, 1000X	47
Figure 14. Alpha Anneal of Ti-6.5 Weight Percent Aluminum Segregation Anneal. 50X, 1000X	48
Figure 15. Segregation Anneal of Ti-9.0 Weight Percent Aluminum Alloy. 50X, 1000X	49

I. INTRODUCTION

In the development of titanium-aluminum base alloys for submarine hull plate material, the Navy has encountered embrittlement in certain alloys resulting in stress corrosion susceptibility in the presence of a notch. This embrittlement was discovered in the Ti-7Al-2Cb-1Ta (Ti-721) alloy by Brown⁽¹⁾ at the Naval Research Laboratory. Lane et al^(2,3) working with titanium-aluminum base alloys found susceptibility to be a function of cooling rate, aging temperature, and aluminum content. These authors are of the opinion that this embrittlement is due to the formation of an ordered compound, Ti_3Al . Cavallaro⁽⁴⁾ found, that by decreasing the aluminum in the Ti-721 alloy to 6 weight percent and adding 0.8 weight percent molybdenum, formation of Ti_3Al can be suppressed, rendering the alloy insensitive to stress corrosion cracking.

Loss of toughness and an increase in strength have been reported^(5,6,7,8) in Ti-Al base alloys when aged in the range of 900-1300°F. Therefore, an embrittling reaction occurs in this temperature range. Present knowledge^(9,10,11) indicates that an ordered compound, Ti_3Al , is the embrittling phase. The exact location of the phase boundaries associated with this compound and its range of solid solubility are still major points of controversy.

Thus, the object of this investigation was to correlate the formation of Ti_3Al , as described by the current phase diagrams^(9,12,13,14,15,16,17,18) to the embrittlement of titanium-aluminum binary alloys. The investigation involved optical metallography, Brown-type stress corrosion tests^(19,20), and Charpy V-notch impact tests⁽²¹⁾.

II. LITERATURE REVIEW

A. Titanium - Aluminum Diagram

The Titanium-Aluminum diagram as originally reported by Ogden et al⁽¹³⁾ and Bumps et al⁽¹²⁾ showed solubility of aluminum in α -titanium extending to more than 20 weight percent at 1470°F. Since that time a number of investigators^(9,16,17,18,22,23) have reported phases other than α below 20 weight percent aluminum. Figure 1 shows the divergence of opinion as to where this extra phase (or phases) exists. This extra phase was initially detected as Superlattice lines on Debye X-ray patterns^(22,24) which indicated the presence of an ordered compound. Ogden and Bumps were not able to detect this ordering because the error in their equipment was of the same order of magnitude as the difference between the lattice parameters of disordered α and the ordered compound. Both α and the ordered compound are hexagonal close packed. The diagrams as seen in Figure 1 have certain significant differences. Ence and Margolin's diagram⁽¹⁶⁾ indicates the presence of two ordered compounds, γ and δ . Clark et al's diagram⁽¹⁷⁾ shows a miscibility gap plus a region containing two ordered compounds α_1' and α_2' . All the diagrams, with the exception of Crossley's⁽⁹⁾ indicate a range of solid solubility for the ordered compound. Also, Crossley's diagram (Figure 2) is the only one which does not indicate a peritectoid reaction of β plus ordered compound going to α . Crossley⁽⁹⁾ reports that the ordered compound, which he identifies as Ti_3Al , has no solid solubility and a closed maximum at about 1605°F. He contends that the other investigators failed to appreciate the difficulty in removing the segregation effects of annealing or working in the $(\alpha + \beta)$ region. Crossley also argued that segregation in the $(\alpha + \beta)$ region results in aluminum-rich and aluminum-lean α -regions which, on cooling, appear as two separate phase regions. X-ray powder patterns should confirm the presence of two hexagonal close packed structures rather than expose the

error because the lattice parameters of hcp α vary significantly with aluminum content.

B. Ti_3Al

Ence and Margolin^(16,24) identified as Ti_2Al a pattern obtained from a powder sample of Ti-25 weight percent aluminum. Reported parameters of this phase were $a = 5.775$ A and $c = 4.638$ A. These parameters are identical to those identified by Clark et al^(17,22), Goldak and Parr⁽²³⁾, and Crossley⁽⁹⁾ as Ti_3Al , a DO_{19} type structure⁽¹¹⁾ (Figure 3). Schroeder⁽²⁵⁾ confirmed the presence of the DO_{19} type structure, which he observed with neutron diffraction studies of alloys containing 8, 15, and 22 weight percent aluminum. The lattice parameters determined by Schroeder were in good agreement with the other investigators. Thus, it appears that the δ phase identified by Ence and Margolin was in reality Ti_3Al , not Ti_2Al .

Ence and Margolin⁽¹⁶⁾ also reported a phase with lattice parameters of $a = 11.52$ A and $c = 4.65$ A. They identified this phase as Ti_3Al (γ phase) from extra lines in their powder patterns. Farrar and Margolin⁽²⁶⁾ as well as other investigators were unable to detect this phase with resistance measurements. Schroeder⁽²⁵⁾ pointed out that the extra lines found by Ence and Margolin could be explained as reflections, caused by stacking faults of the ordered lattice. He also pointed out that line intensities of superlattice lines are a function of ordering, $S = \frac{r_a - F_a}{1 - F_a}$ where r_a is the fraction of A-sites

occupied by A- atoms and F_a is the fraction of A-atoms in the alloy. His theoretical calculations showed, that for $S=0.5$, the 101 line of the ordered lattice (with d-spacing of about 3.4 A) will appear as the strongest superlattice line, while at complete ordering ($S=1$) the 110 line will appear four times stronger than the 101 line. Thus, Ence and Margolin may not have taken into consideration the degree of ordering in their analysis. Therefore, a phase with the hcp lattice parameters of $a=11.52$ A and $c=4.65$ A as described by Ence and Margolin appears not to exist.

C. Ordering and Embrittlement

Among the potential metallurgical reasons for ordering are size factor, electronegativity, relative valency, and chemical affinity. Extensive substitutional alpha solubility is restricted to elements having size factors within ten percent⁽²⁷⁾ of titanium. The aluminum atom is only about three percent smaller than the titanium atom yet the titanium-aluminum system exhibits three ordered compounds (Ti_3Al , $TiAl$, $TiAl_3$). Thus size factor does not enter into the ordering reaction. The electronegativity⁽²⁷⁾ of titanium and aluminum are essentially the same. Ordinarily, of course, compound forming tendencies increase with increasing difference in electronegativity.

The importance of the relative valency effect and electron concentration are less well known because the alloying valences of the transition metals (titanium is a transition metal) are not well understood. Pauling⁽²⁸⁾ assigns a metallic valence of four to titanium whereas Denny⁽²⁹⁾ presents evidence in favor of a metallic valence of about 1.5. For non-transition metals, the relative valency effect⁽³⁰⁾ may be described by saying that a metal of lower valency tends to dissolve a metal of higher valency more readily than vice versa. However, the general validity of this statement for transition metals may be questioned on the grounds that their metallic valences are not well known and are probably not constant. Be that as it may, Table I shows the solubilities of transition elements in aluminum and aluminum solubilities in them.⁽³¹⁾ That aluminum is extensively soluble in transition elements while the reverse is not true could mean that titanium and the transition metals as a group all have effective valences less than three when alloyed with aluminum and this supports Denny's conclusion that the metallic valence of titanium is about 1.5. Nevertheless, the situation with regard to metallic valence and electron concentration provides no real clues with regard to the ordering tendency.

With regard to the chemical affinity effect, the work of Kubaschewski et al^(32,33) disclosed significant heats of formation

in the Ti-Al system and his data are shown in Figure 4. As may be seen, the enthalpy of alloying is significant even at 8 weight percent aluminum. These results lead to the conclusion that there is a strong chemical affinity between titanium and aluminum.

Blackburn's recent work⁽¹⁰⁾ on the Ti-8Al-1Mo-1V and Ti-Al systems, using transmission electron microscopy, showed that ordered domains of Ti_3Al restricted cross slip and reduced the rate of work hardening. Thus, embrittlement could be correlated to restricted cross slip because coplanar arrays of dislocations might nucleate microcracks at pile-ups against brittle domains of Ti_3Al .

III. EXPERIMENTAL PROCEDURE

A. Material

Twenty-five gram buttons of Titanium- 4.1 weight percent (7 atomic percent), - 6.5 weight percent (11 atomic percent), and - 9.0 weight percent (15 atomic percent) aluminum were prepared in a non-consumable electrode arc melting furnace for metallographic study. Materials used in the preparation of the alloys are given in Table II. Buttons were remelted three times for homogeneity. Nominal compositions of buttons was taken as correct because weight loss after melting was no greater than 10 mg for any alloy button.

Ti-Al alloys of 5 weight percent (8.5 atomic percent), 6 weight percent (10.2 atomic percent), 7 weight percent (11.8 atomic percent), and 8 weight percent (13.4 atomic percent) aluminum were prepared by Titanium Metals Corporation of America in the form of hot forged bars. Chemical analysis of these alloys and their forging temperatures are given in Table III. Metallographic, stress corrosion, and Charpy V-notch impact specimens were made from these bars.

B. Heat Treatment

Specimens for metallographic study were encapsulated in quartz tubes. The tubes were flushed with argon three times before the final sealing off of the tubes under vacuum.

Blanks to be machined into stress corrosion and Charpy specimens were heat treated in a vacuum-annealing furnace unless water quenching was part of the thermal treatment. When water quenching was required, the blanks were heat treated in a regular atmosphere furnace. To minimize atmospheric contamination, the blanks were coated with a ceramic designated as CR T-22 by the manufacturer, Markal. The composition of this ceramic is not disclosed by the manufacturer.

Thermal treatments given all alloys for stress corrosion and Charpy V-notch impact tests may be grouped into three types. These treatments are listed below:

1. As-received or β -forged

2. 2200°F- 1 hour- water quenched (β region)
+ 1650°F- 1 hour- water quenched (α region)
3. Same as treatment Number 2 + aging at 1100°F- 2 hours- air cool (α + Ti₃Al region)

For alloys containing 5 and 7 weight percent aluminum, two additional treatments which are shown below were used:

4. 2200°F- 1 hour- water quenched (β region)
+ 1830°F(5 weight percent)-2 hours-water quenched ($\alpha + \beta$)
+ 1880°F(7 weight percent)-2 hours-water quenched region
5. Same as above plus aging at 1100°F for various times.

C. Metallography

Metallographic specimens were mounted in bakelite and rough-polished through 600 grit emery paper. Final polishing was performed with a Buehler electrolytic polishing cell, Model No. 1721-2AB. The electrolyte⁽³⁴⁾ used was a mixture of 60 ml perchloric acid, 350 ml butyl cellosolve, and 590 ml ethyl alcohol. The polishing time was approximately 45 seconds at a potential of 36 volts and a current of 0.2-0.4 amperes. The specimens were then etched in a solution of one part sulfuric acid, two parts hydrofloric acid, three parts nitric acid, and 94 parts distilled water.

D. Stress Corrosion and Charpy V-notch Impact Tests

The "Brown-type"^(19,20) cantilever beam stress corrosion test was used throughout this study (Figure 5). This test employs a pre-cracked bar specimen exposed to a corrosive media. This test provides an accelerated method of evaluating stress corrosion susceptibility. Time required to form a pit and for the pit to attain sufficient depth and acuity for stress corrosion cracking is eliminated by this method of testing. This test also reveals stress corrosion susceptibility in alloys, such as titanium alloys, which do not form a pit; but will stress corrode once a surface stress concentration exists. Notched specimens 0.420 inches square x 5 inches long were tested in air and in seawater obtained from Harbor Island, North Carolina. A reser-

voir was used for the tests conducted in sea water. The notch was machined at the midlength of the specimen perpendicular to the rolled surface to a depth of 20 percent of the specimen thickness. The machined notch contained a root radius of 0.002 inches. Some specimens were tested with only the machined notch, but most were fatigue-cracked using a Manlabs fatigue pre-crack machine, to achieve a total defect depth (machined notch plus fatigue crack) of 25 to 35 percent of the specimen depth. The specimen was stressed by step loading after exposure to seawater. Loading was in increments to produce a nominal stress increase of 10 to 15 ksi at the notch. These incremental stress increases were made at 5-minute intervals until rupture by adding lead shot to a bucket fixed at the end of a moment arm. Tests in air were run using the same technique. Companion samples were tested in air and in seawater for each alloy and heat treatment considered. Duplicate tests were made whenever possible.

A nominal bending stress to fracture was calculated at the notch root⁽²⁰⁾ using simple beam theory, $\sigma^n = \frac{Mc}{I}$. A ratio of the fracture stress in seawater over the fracture stress in air was used as a parameter of the sensitivity of a material to stress corrosion. Figure 6 illustrates a typical cross section of an embrittled specimen.

Standard Charpy V-notch impact specimens, as specified by ASTM⁽²¹⁾, were run as a measure of toughness. Impact tests were performed in a Riehle, Model PI-2, impact testing machine. The testing temperature was 32°F. Duplicate specimens were run for each alloy and heat treatment.

IV. RESULTS AND DISCUSSION

A. Metallography

Titanium-aluminum alloys in the as-arc-melted condition consists of large equiaxed grains of α . A typical structure is shown in Figure 7. The as-received hot forged structure of Ti-Al alloys is shown in Figure 8 and consists of Widmanstätten α .

An 8 weight percent aluminum alloy was annealed for 6 hours at 1100°F after a prior β -anneal. This temperature is in the $\alpha + \text{Ti}_3\text{Al}$ region according to Crossley⁽⁹⁾. At 1000x magnification, a precipitate can be seen at the platelet boundaries (Figure 9). A portion of this specimen was reannealed at 1650°F for 20 hours and air cooled. This re-annealing resulted in the solution of the precipitate (Figure 10). Another portion of the specimen was annealed at 1650°F for 64 hours and water-quenched. This treatment resulted in the martensitic reaction of α to γ' at the prior platelet boundaries. The martensitic form of Ti_3Al is γ' . This reaction indicated that these areas remained rich in aluminum after annealing (Figure 11). Crossley⁽⁹⁾ has shown that the α to γ' reaction does not occur on quenching in alloys containing less than 9 weight percent aluminum.

Segregation effects are apparent in alloys heat treated in the ($\alpha + \beta$) region. This segregation is illustrated in Figures 12, 13, and 15 for alloys containing 4.1, 6.5, and 9.0 weight percent aluminum, respectively. Prior β -grains transformed to Widmanstätten α during the heat treatment. The interface between α and prior β in the Ti-6.5 weight percent aluminum alloy was enriched sufficiently in aluminum to cause the precipitation of Ti_3Al on furnace cooling.

Figures 14 and 16 show the microstructures of 6.5 and 9.0 weight percent aluminum alloys after annealing was attempted to remove the segregation. The alloy containing 6.5 weight percent aluminum was annealed at 1650°F for 48 hours, while the 9.0 weight percent aluminum alloy was annealed at 1850°F for 240 hours. Both treatments

were in the α -region just below the α -transus. The heat treatment removed segregation for the most part in the 9.0 weight percent aluminum alloy (Figure 16). However, after this second treatment, segregation was still noticeable in the 6.5 weight percent aluminum alloy (Figure 14).

Because the Ti_3Al present in the Ti-8 weight percent aluminum alloy could be dissolved by annealing at $1650^{\circ}F$ indicates that the diagrams of Sagel⁽¹⁵⁾ and Ence and Margolin⁽¹⁶⁾ are in error. Their diagrams indicated that a two phase field exists at this composition and temperature.

The existence of high aluminum content at platelet boundaries after long anneals at $1650^{\circ}F$ (8 weight percent aluminum alloy) together with long annealing times required to remove segregation in the 6.5 and 9.0 weight percent aluminum alloys seem to validate Crossley's arguments. According to Crossley, other investigators did not fully appreciate the difficulty of removing the segregation effects of working or annealing in the ($\alpha + \beta$) field. All other investigators^(14,15,16,17,18) with the exception of Bumps et al⁽¹²⁾ and Ogden et al⁽¹³⁾, either worked or annealed their specimens in the ($\alpha + \beta$) region. Bumps and Ogden, of course, did not report the presence of a two-phase field below the α -transus.

Although the alloys studied went no higher than 9.0 weight percent aluminum, indications are given as to the validity of Crossley's diagram. It is obvious that it is extremely hard to homogenize a segregated structure below the α -transus. It can readily be seen that some two phase regions reported by other investigators at temperatures below the α -transus could be the result of segregation remaining in the structure. Although the question of whether Ti_3Al is an ordered compound or an ordered solid solution with a range of solubility has not been resolved, Crossley⁽³⁵⁾ has shown that Ti_3Al can be overaged in an equiaxed α structure (Figure 17), resulting in the regaining of impact strength. This would suggest that Ti_3Al is an ordered compound with no range of solid solubility.

B. Stress Corrosion and Charpy V-notch Impact Tests

Four alloys containing 5,6,7, and 8 weight percent aluminum were given various heat treatments, as described in section III, in an effort to determine the effects of thermal treatments and aluminum content on toughness and stress corrosion susceptibility. Results of this investigation are shown in Tables IV thru VII.

Alloys given an α -treatment after the prior β -anneal (Treatment #2) showed an increase in both toughness and in resistance to stress corrosion when compared to the β -forged condition. In general the properties of the alloys improved with this treatment. The additional treatment of aging at 1100°F caused an increase in the stress corrosion susceptibility and a loss in toughness. Aging produced properties of the order of those found in the β -forged specimens. For all treatments, stress corrosion susceptibility increased and toughness decreased as the aluminum content increased from 5 to 8 weight percent aluminum.

Alloys containing 5 and 7 weight percent aluminum were treated in the ($\alpha + \beta$) region after β -annealing. This treatment resulted in a decrease in stress corrosion susceptibility without much change in toughness compared to the β -forged condition. However, these properties after treatment in the ($\alpha + \beta$) region are much less than those found in the α -annealed state.

The additional treatment of aging at 1100°F for various times after treatment in the ($\alpha + \beta$) region had a detrimental effect on the properties of these alloys. Short aging times resulted in a slight increase in stress corrosion susceptibility and a decrease in toughness when compared to the non-aged condition. Longer aging times out to 70 hours showed a further decrease in stress corrosion resistance and toughness. Further aging had no effect. Properties of the ($\alpha + \beta$) treated plus aged alloys were lower than the same properties in the β -forged state.

The results indicate that up to 8 weight percent aluminum,

no embrittlement resulted from a 1650°F anneal after a β -anneal. Thus, up to 8 weight percent aluminum, a single phase region exists at this temperature of 1650°F.

The β -anneal plus α -anneal results in a Widmanstätten structure. The aluminum enriched Widmanstätten plates form Ti_3Al quite readily when held in the ($\alpha + Ti_3Al$) region as was observed in the metallographic study. Besides forming Ti_3Al quite readily in the plate boundaries, the Widmanstätten structure provides a relatively continuous path for stress corrosion cracking. The ($\alpha + \beta$) annealed structure required much greater annealing times at 1100°F to induce stress corrosion susceptibility. This too can be related to structure. The ($\alpha + \beta$) anneal results in equiaxed α -grains and transformed β -grains (Widmanstätten α). In the equiaxed α -grains, time is required for aluminum atoms to diffuse to ordered sites. A three hour age at 1100°F had little effect in reducing stress corrosion resistance in the 7 weight percent aluminum alloy (Table VI) after an ($\alpha + \beta$) anneal. Increasing the aging time of this alloy to 70 hours, however, resulted in a drastic loss in stress corrosion resistance. The 5 weight percent aluminum alloy (Table IV) did not become susceptible to stress corrosion regardless of aging time (up to 168 hours) indicating that the Ti_3Al precipitate is more dispersed in an equiaxed α -structure. Thus a greater aluminum content is needed for precipitation in equiaxed α -structure to form a path for stress corrosion than would be required in a Widmanstätten structure. The 5 weight percent aluminum alloy became susceptible to stress corrosion on aging only when the Widmanstätten structure was present (β anneal + α anneal).

Toughness decreased significantly on aging the Widmanstätten structure but not in proportion to the loss of stress corrosion resistance. Toughness decreased with time after an ($\alpha + \beta$) anneal. The 7 weight percent aluminum alloy aged 70 hours after an ($\alpha + \beta$) anneal showed a drastic loss in toughness as did stress corrosion resistance. The 5 weight percent aluminum alloy showed a continuous

decrease in toughness with aging time without a corresponding loss in stress corrosion resistance. Thus, there seems to be a difference in the effect of precipitation of Ti_3Al on stress corrosion and toughness. It can be concluded from aging the 5 and 7 weight percent aluminum alloys after an ($\alpha + \beta$) anneal that a critical amount of Ti_3Al must precipitate in an equiaxed α -structure before stress corrosion susceptibility becomes a problem, whereas, loss of toughness seems to be simply a function of the amount of Ti_3Al forming. On the basis of this observation, it is proposed that loss of toughness is a result of the precipitate acting as a barrier to dislocation movement. Stress corrosion, however, appears to be a combination of electrochemical factors, requiring a relatively continuous path of precipitate, and restricted slip.

V. CONCLUSIONS

The following conclusions can be drawn from this investigation of Ti-Al alloys in the composition range of 5 to 9 weight percent aluminum:

1. The segregation effects of annealing in the ($\alpha + \beta$) region are extremely difficult to remove below the α -transus.
2. Optimum stress corrosion resistance and toughness are obtained from a β anneal plus α anneal without aging. These properties are drastically reduced when the alloy is subsequently annealed in the ($\alpha + \text{Ti}_3\text{Al}$) region for short periods of time. Toughness is less affected by aging than is stress corrosion resistance.
3. The Widmanstätten platelet boundaries are enriched in aluminum and the ordered precipitate forms quite readily when held in the ($\alpha + \text{Ti}_3\text{Al}$) region. The β anneal plus α anneal results in a Widmanstätten structure.
4. As a result of the precipitation of Ti_3Al in platelet boundaries on aging, the Widmanstätten structure provides a continuous path for stress corrosion cracking.
5. Long annealing times are required to induce stress corrosion susceptibility in Ti-Al alloys after an ($\alpha + \beta$) anneal because time is required for aluminum atoms to diffuse to ordering sites in equiaxed α -grains which result from the ($\alpha + \beta$) anneal.
6. Greater amounts of aluminum content are required to induce stress corrosion susceptibility after an ($\alpha + \beta$) anneal because the precipitate is more dispersed in equiaxed structure than in Widmanstätten structure where Ti_3Al is concentrated in platelet boundaries.
7. After an ($\alpha + \beta$) anneal, toughness decreases with annealing time when held in the ($\alpha + \text{Ti}_3\text{Al}$) region. Toughness will

be adversely affected by aging at lower aluminum contents than will stress corrosion resistance.

VI. FUTURE WORK

Consideration in future work should be given to the effects of ternary additions to the Ti-Al system on promoting or suppressing the formation of Ti_3Al . Suppression of the Ti_3Al reaction would enable the use of higher aluminum contents for strength without a loss in toughness and stress corrosion resistance.

The Ti-Al diagram itself should be investigated further. The controversy of whether or not Ti_3Al is an ordered solid solution or an ordered compound should be resolved. The question as to whether a peritectoid reaction of ordered compound plus β going to α should also be investigated further.

VII. BIBLIOGRAPHY

1. Brown, B.F., "Progress in the Development of Test Concepts for Stress Corrosion Cracking," NRL Tech Memo 6320-44, Naval Research Laboratory, Washington D.C, December 1964.
2. Lane, I.R., Cavallaro, J.L., and Morton, A.G.S., "Fracture Behavior of Titanium in the Marine Environment," MEL Phase Report 231/65, U.S.N. Marine Engineering Laboratory, Annapolis, Md., July 1965.
3. Lane, I.R., Cavallaro, J.L., and Morton, A.G.S., "Sea Water Embrittlement of Titanium," American Society for Testing and Materials Special Technical Publication No. 397, 1966, pp.246
4. Cavallaro, J.L., "Ti-6Al-2Cb-1Ta-0.8Mo Titanium Alloy as a Structural Material for Marine Applications," MEL Phase Report 506/66, U.S.N. Marine Engineering Laboratory, Annapolis, Md., January 1967.
5. Crossley, F.A. and Carew, W.F., "Embrittlement of Ti-Al Alloys in the 6-10 Weight Percent Range," Transactions of the Metallurgical Society of AIME, 209, 1957, pps. 43-46.
6. Willner, A.R., and Salive, M.L., "The Effects of Temperature, Time, and Cooling Rate on the Mechanical Properties of 8Al-2Cb-1Ta Titanium Alloy," Technical Note SML720-30, David Taylor Model Basin, Carderock, Md., March 1963.
7. Seagle, S.R., DeBlasio, L.R., and Berteau, O., "Processing Study of Ti-7Al-2Cb-1Ta," Reactive Metals Inc., Niles, Ohio, Final Report to U.S.N. Marine Engineering Laboratory, Contract No. N161-25741, February 1965.
8. Wolff, A.K., Aronin, L.R., and Abkowitz, S., "Development of Titanium Alloys for Deep-Diving Vehicles," Nuclear Metals, West Concord, Mass., Final Report to U.S.N. Marine Engineering Laboratory, Contract No. N600(61533)59922, May 8, 1964.

9. Crossley, F.A., "Titanium-Rich End of the Titanium-Aluminum Diagram," Transactions of the Metallurgical Society of AIME, 236, 1966, pps. 1174-1185.
10. Blackburn, M.J., "Phase Transformations in the Alloy Ti-3Al-1Mo-1V," Boeing Report No. DL-82-0402, Boeing Scientific Research Laboratories, Seattle, Washington, January 1965.
11. Portisch, H. and Margolin, H., "A Study of the Crystal Structure of Ti-Al Alloys and Hydrogen Induced Expansions," New York University School of Engineering and Science, Research Division, Contract No. DA-ARO(D)-31-124-G519 for U.S. Army Research Office, September 1966.
12. Bumps, E.S., Kessler, H.D., and Hansen, M., "Titanium-Aluminum System," Transactions of the Metallurgical Society of AIME, 194, 1952, pps. 609-614.
13. Ogden, H.R., Maykuth, D.J., Finlay, W.L., and Jaffee, R.I., "Constitution of Titanium-Aluminum Alloys," Transactions of the Metallurgical Society of AIME, 191, 1951, pps. 1150-1155.
14. Sato, T., and Huang, Y., "The Equilibrium Diagram of the Ti-Al System," Transactions Japan Institute of Metals, 1, 1960, pps. 22-27.
15. Sagel, K., Schulz, E., and Zwicker, U., "Untersuchungen am System Titan-Aluminum," Z. Metallkunde, 46, 1956, pp. 529.
16. Ence, E. and Margolin, H., "Phase Relations in the Titanium-Aluminum System," Transactions of the Metallurgical Society of AIME, 221, 1961, pps. 151-157.
17. Clark, D., Jepson, K.S., and Lewis, G.I., "A Study of the Titanium-Aluminum System Up to 40 Atomic Percent Aluminum," Journal of the Institute of Metals, 91, 1962-1963, pp. 197.
18. Tsujimoto, T., and Adachi, M., "Reinvestigation of the Titanium-Rich Region of the Titanium Aluminum Diagram," Journal of the Institute of Metals, 94, 1966, pps. 358-363.

19. Brown, B.F., "A New Stress Corrosion Cracking Test for High Strength Alloys," Materials Research and Standards, Vol. 6, No. 3, March 1966, pps. 129-133.
20. Brown, B.F., and Beachen, C., "A Study of the Stress Factor in Corrosion Cracking by Use of the Pre-Cracked Cantilever Beam Specimen," Paper presented in Brussels, Belgium (7-11 June 1965) during Corrosion Week.
21. Charpy V-notch Impact Test, ASTM Standards 1958, Part 3-Methods of Testing, pps. 73-75.
22. Clark, D. and Terry, J.C., "Superlattice Formation in the Alpha Titanium-Aluminum Solid Solutions," Institute of Metals Bulletin, 3, 1956, pp. 116.
23. Goldak, A.J. and Parr, G., "The Structure of Ti_3Al ," Transactions of the Metallurgical Society of AIME, 221, 1961, pps. 639-640.
24. Ence, E. and Margolin, H., "Compounds in the Titanium-Rich Region of the Titanium-Aluminum System," Transactions of the Metallurgical Society of AIME, 209, 1957, pps. 484-485.
25. Schroeder, J., "Investigation of the Ordered Phase Ti_3Al ," M.S. Thesis, Ohio State University.
26. Farrar, P.A. and Margolin, H., "A Study of the Factors Affecting the Decomposition of the Intermediate Phase Ti_3Al ," New York University, Technical Report AFML-TR-65-69, Sponsored by Air Force Materials Laboratory, Wright Patterson Air Force Base, Ohio, June 1965.
27. Maykuth, D.J., Ogden, H.R., and Jaffee, R.I., "The Effects of Alloying Elements in Titanium, Volume A Constitution," DMIC 136A, Battelle Memorial Institute, Columbus, Ohio, 1960.
28. Pauling, L., The Nature of the Chemical Bond, Third Edition, Cornell University Press, 1960
29. Denny, J.M., "A Study of Electron Effects in Solid Solution Alloys of Titanium, California Institute of Technology, 6th Technical Report to Office of Naval Research on Contract No.

N6Onr 24430, January 1955.

30. Cottrell, A.H. , Theoretical Structural Metallurgy, Edward Arnold Ltd., London, England, 1962, pp. 128
31. Hansen, M., Constitution of Binary Alloys, Second Edition, McGraw Hill Book Company, New York, New York, 1958.
32. Kubaschewski, O., Wainwright, C., and Kirby, F.J., "The Heats of Formation in the Ti-Al-V System," Journal of the Institute of Metals, 89, 1960, pps. 139-144.
33. Kubaschewski, O., and Dench, W.A., "The Heats of Formation in the Systems Ti-Al and Ti-Fe, Acta Metallurgica, 3 , 1955, pps. 339-346.
34. Crossley, F.A., Private communication with Mr. I.R. Lane, U.S.N. Marine Engineering Laboratory, Annapolis, Maryland, 1967.
35. Ogden, H.R. and Holden, F.C., "Metallography of Titanium Alloys, TML Report No. 103, Battelle Memorial Institute, Columbus, Ohio, May 29, 1958.

VIII. ACKNOWLEDGEMENTS

The author is deeply indebted to his co-workers at the U.S.N. Marine Engineering Laboratory, especially to Messrs. I.R. Lane, J.L. Cavallaro, A.G.S. Morton, Arthur Robson, and John Sydavar for their advice and guidance.

The author also expresses thanks for the consideration and help given to him by Dr. Roy Wilcox of the Department of Metals and Ceramics at the Virginia Polytechnic Institute.

**The vita has been removed from
the scanned document**

TABLE I

MUTUAL SOLID SOLUBILITIES OF ALUMINUM AND TRANSITION ELEMENTS

SOLID SOLUBILITIES, ATOMIC PERCENT

	Ti	V	Cr	Mn	Fe	Co	Ni	Zr	Mo	Pd	W
Maximum Solubility in Aluminum	0	0.2	1	1	0	0	0	0	0	0	0
Maximum Solubility Aluminum in	42	50	56	22	54	16	21	26	19	18	15

FIGURE 4- RELATIONSHIP OF MUTUAL SOLUBILITY OF
ALUMINUM AND TRANSITION ELEMENTS

TABLE II

Composition of Titanium Sponge and Aluminum Shot
Used to Prepare Alloy Buttons

Titanium Sponge	
Chemical Analyses	Spectrographic Analyses
.033 % O ₂	.033 % Cr
.005 % N ₂	.001 % Mo
.005 % H ₂	.001 % Al
.013 % C	.010 % V
.091 % Cl ₂	.020 % Sn
.010 % Fe	.007 % Mn
.015 % H ₂ O	.001 % Mg
.002 % Si	.001 % Ni
72.8 Bhn at 1500 Kg loading with 10mm ball	.002 % Cu
	.001 % Zr
	.001 % B
Chemical Analyses of Aluminum Shot	
99.993 % Purity	

TABLE III

Data on Ti-Al Alloy Forgings

Nominal Composition wt. %	Forging Temperature °F	Al wt. %	Fe wt. %	O wt. %	N wt. %
Ti-5Al	2000	5.05	0.054	0.075	0.006
Ti-6Al	2100	6.08	0.038	0.097	0.006
Ti-7Al	2100	7.16	0.031	0.076	0.012
Ti-8Al	2200	8.39	0.031	0.062	0.010

TABLE IV

STRESS CORROSION AND IMPACT DATA FOR 5 WEIGHT
PERCENT ALUMINUM

HEAT TREATMENT	Envir- onment	Frac- ture Stress ksi	Notch	S_n (SW)	Charpy V- Notch Im- pact Str. ft.-lb.
				S_n (Air) (1)	
As received (Hot Forged- 2000°F)	Sea Water	164	0.002R	0.78	41
	Air	213			
2200°F-1 hr.-WQ +1650°F-1 hr.-WQ	Sea Water	188	0.002R + F.C.*	0.93	46
	Air	203			
2200°F-1 hr.-WQ +1650°F-1 hr.-WQ +1100°F-2 hr.-AC	Sea Water	160	0.002R + F.C.	0.71	39
	Air	224			
2200°F-1 hr.-WQ +1830°F-2 hr.-WQ	Sea Water	175	0.002R + F.C.	0.83	40
	Air	210			
2200°F-1 hr.-WQ +1830°F-2 hr.-WQ +1100°F-26 hr.-AC	Sea Water	168	0.002R + F.C.	0.81	35
	Air	208			
2200°F-1 hr.-WQ +1830°F-2 hr.-WQ +1100°F-70 hr.-AC	Sea Water	162	0.002R + F.C.	0.76	27
	Air	212			
2200°F-1 hr.-WQ 1830°F-2hr.-WQ 1100°F-168hr.-AC	Sea Water	159	0.002R + F.C.	0.76	24
	Air	207			

* F.C. = Fatigue Crack

$$(1) \frac{S_n(SW)}{S_n(Air)} = \frac{\text{Fracture Stress in Sea Water}}{\text{Fracture Stress in Air}}$$

TABLE V
STRESS CORROSION AND IMPACT DATA FOR 6 WEIGHT
PERCENT ALUMINUM

HEAT TREATMENT	Environment	Fracture Stress ksi	Notch	S_n (SW)	Charpy V-Notch Impact Str ft.-lb.
				S_n (Air)	
As received (Hot Forged- 2100 F)	Sea Water	130	0.002R	0.65	34
	Air	200			
2200°F-1 hr.-WQ +1650°F-1 hr.-WQ	Sea Water	164	0.002R + F.C.	0.89	44
	Air	184			
2200°F-1 hr.-WQ +1650°F-1 hr.-WQ +1100°F-2 hr.-AC	Sea Water	135	0.002R + F.C.	0.62	35
	Air	217			

TABLE VI

STRESS CORROSION AND IMPACT DATA FOR 7 WEIGHT

PERCENT ALUMINUM

HEAT TREATMENT	Envir- onment	Frac- ture Stress KSI	Notch	$\frac{S_n(SW)}{S_n(Air)}$	Charpy V- Notch Impact Str. ft.-lb.
As received (Hot Forged - 2100°F)	Sea Water	100	0.002R	0.51	26
	Air	197			
2200°F-1 hr.- WQ +1650°F-1 hr.- WQ	Sea Water	210	0.002R + F.C.	0.98	34
	Air=	215			
2200°F-1 hr.- WQ +1650°F-1 hr.- WQ +1100°F-2 hr.- AC	Sea Water	95	0.002R + F.C.	0.48	25
	Air	195			
2200°F-1 hr.- WQ +1880°F-1 hr.- WQ	Sea Water	170	0.002R + F.C.	0.92	30
	Air	185			
2200°F-1 hr.- WQ +1880°F-1 hr.- WQ +1100°F-3 hr.- AC	Sea= Water	160	0.002R + F.C.	0.89	21
	Air	179			
2200°F-1 hr.- WQ +1880°F-1 hr.- WQ +1100°F-70 hr.-AC	Sea Water	69	0.002 + F.C.	0.39	14
	Air	175			
2200°F-1 hr.- WQ +1880°F-1 hr.- WQ +1100°F-100hr.-AC	Sea Water	68	0.002R + F.C.	0.39	13
	Air	176			

TABLE VII
 STRESS CORROSION AND IMPACT DATA FOR 8 WEIGHT
 PERCENT ALUMINUM

HEAT TREATMENT	Environment	Fracture Stress ksi	Notch	$\frac{S_n(SW)}{S_n(Air)}$	Charpy V-Notch Impact Str ft.-lb.
As received (Hot Forged- 2200°F)	Sea Water	80	0.002R	0.54	18
	Air	150			
2200°F-1 hr.- WQ +1650°F-1 hr.- WQ	Sea Water	135	0.002R + F.C.	0.84	20
	Air	161			
2200°F-1 hr.- WQ +1650°F-1 hr.- WQ +1100°F-2 hr.- AC	Sea Water	82	0.002R + F.C.	0.52	17
	Air	159			

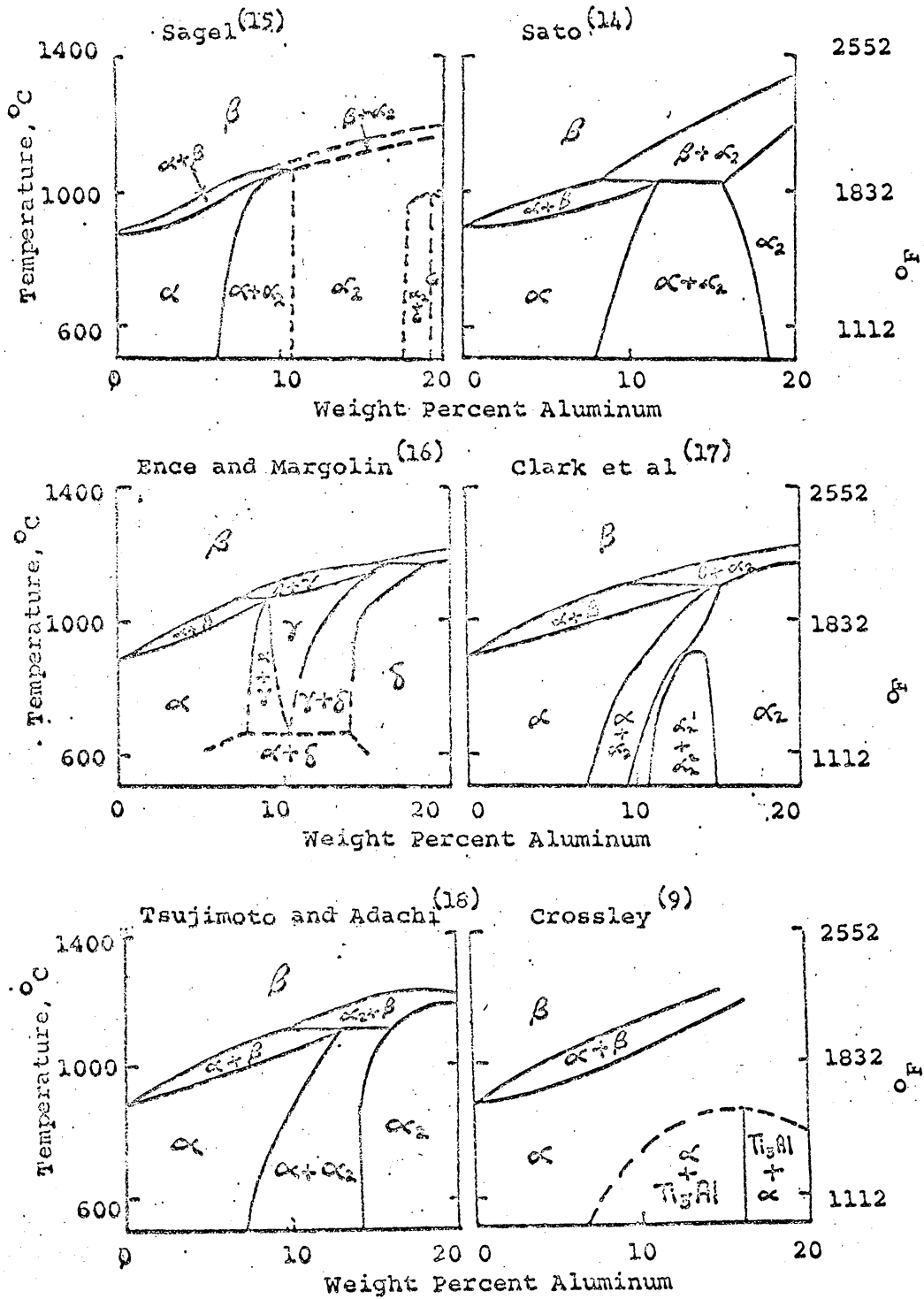


FIGURE 1 - Comparison of Proposed Ti-Al Diagrams

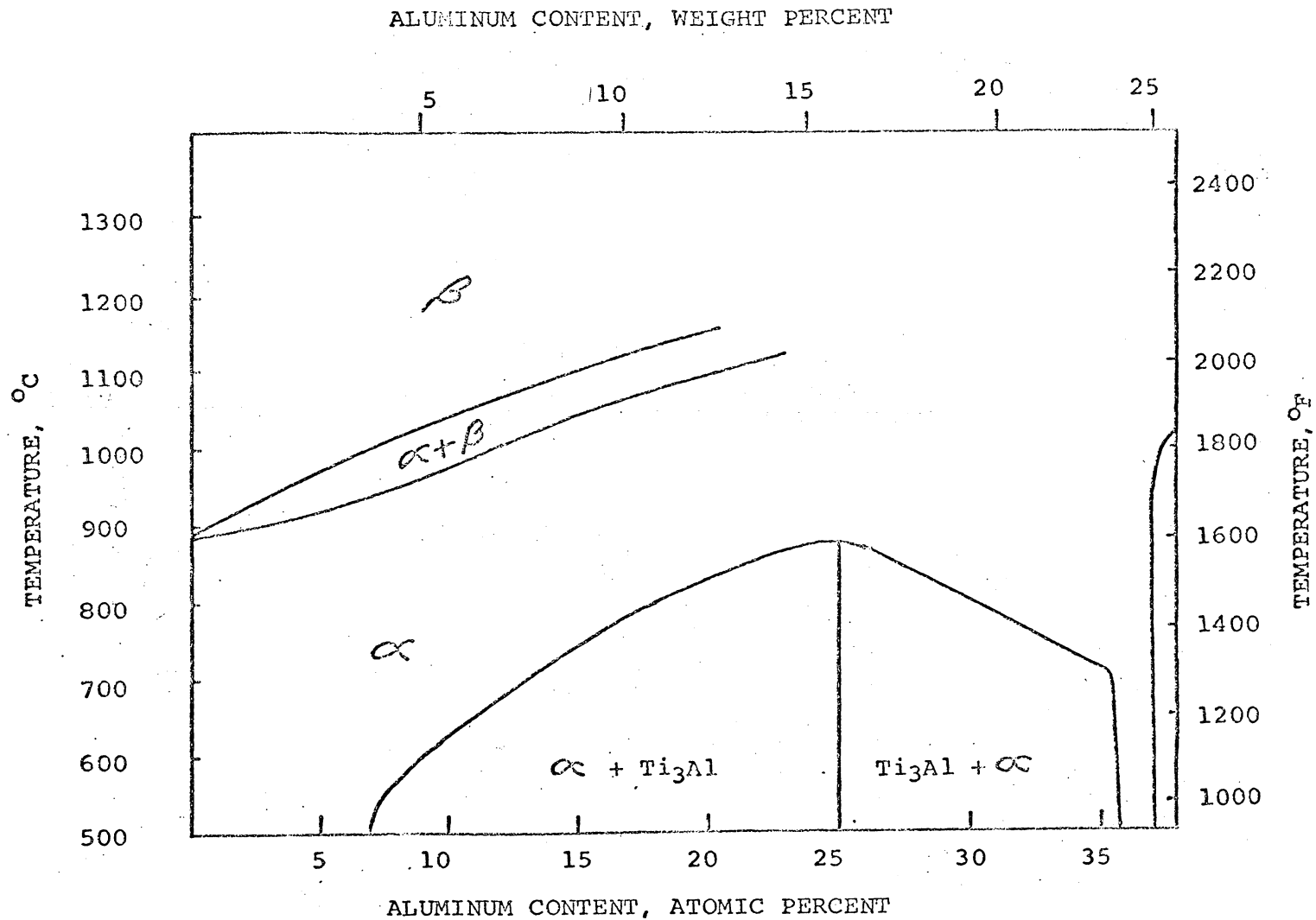


FIGURE 2- TITANIUM-RICH END OF THE Ti-Al SYSTEM (9)

KEY:

LOCATION:
 C_0 -LENGTHS ABOVE
 PLANE OF PAPER

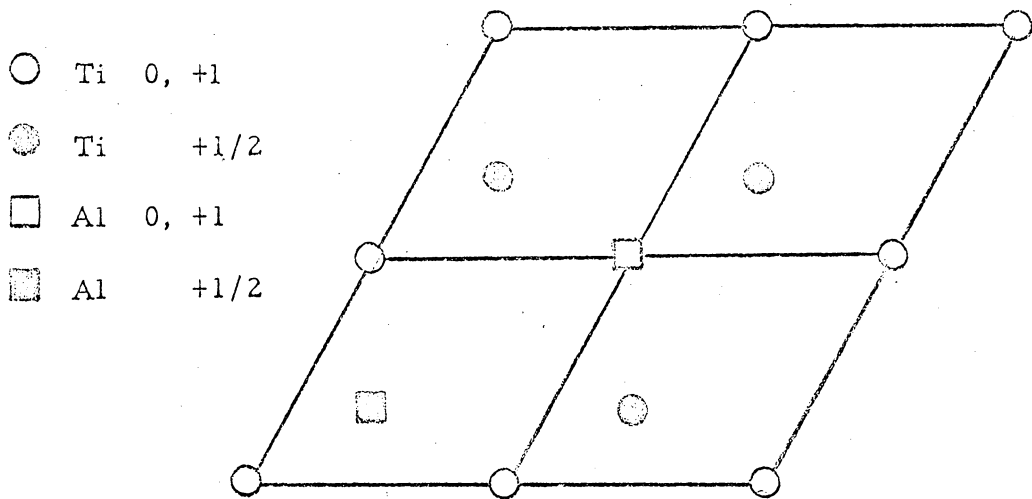


Figure 3. DO_{19} structure of Ti_3Al (Mg_3Cd type structure)⁽¹¹⁾

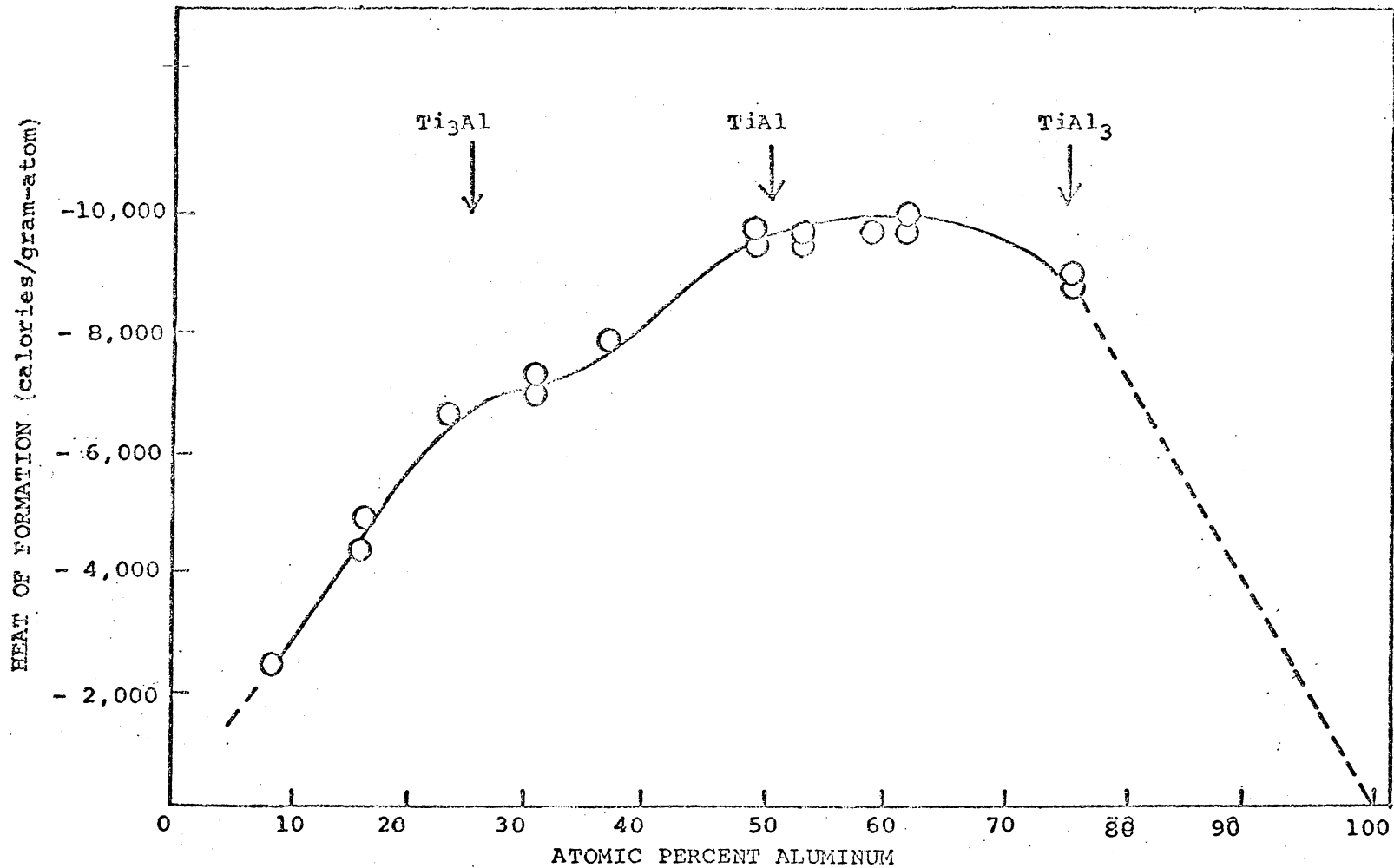


FIGURE 4 - HEATS OF FORMATION OF ALLOYS IN Ti-Al SYSTEM (33)

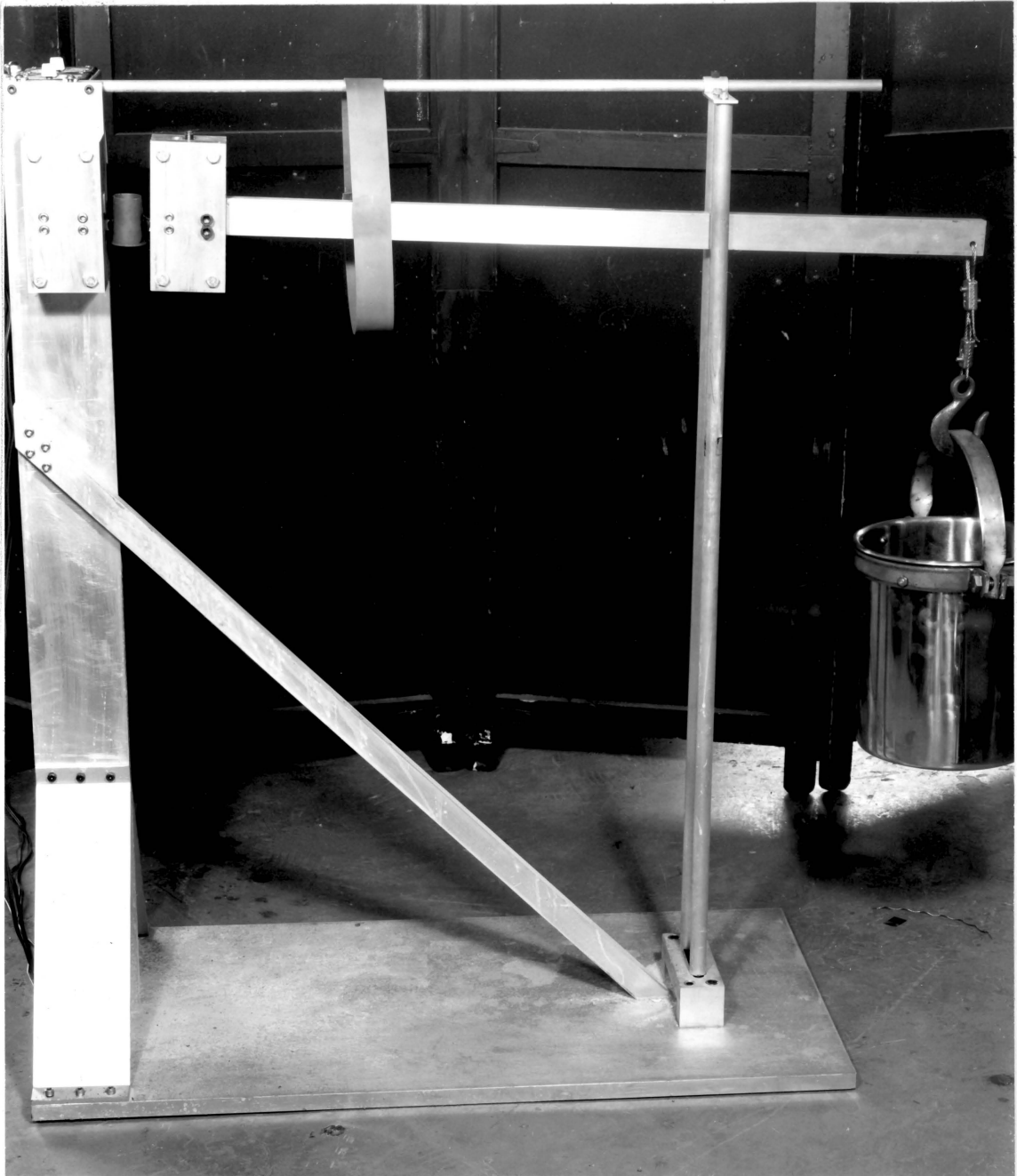


Figure 5. Brown Type Stress Corrosion Test Apparatus.

- ① - Machined Notch
- ② - Fatigue Crack
- ③ - Embrittled Zone
- ④ - Air Type Mechanical Fracture Zone

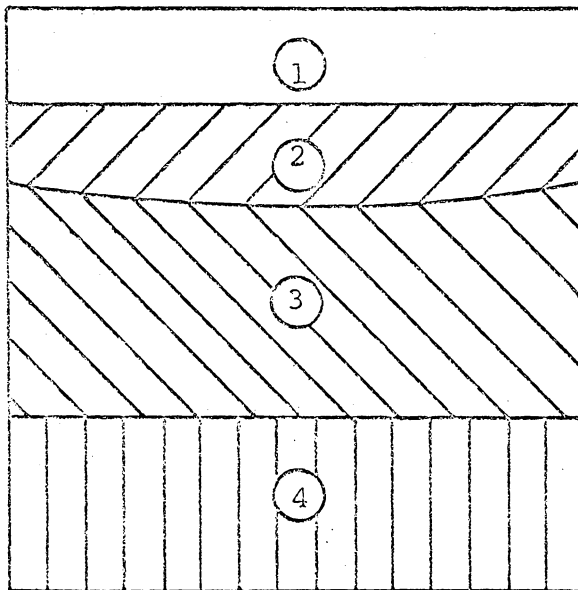


FIGURE 6 - VARIOUS ZONES THAT APPEAR IN THE FRACTURED SURFACE OF TITANIUM ALLOYS AFTER EXPOSURE TO STRESS IN A MARINE ENVIRONMENT IN THE PRESENCE OF A FLAW

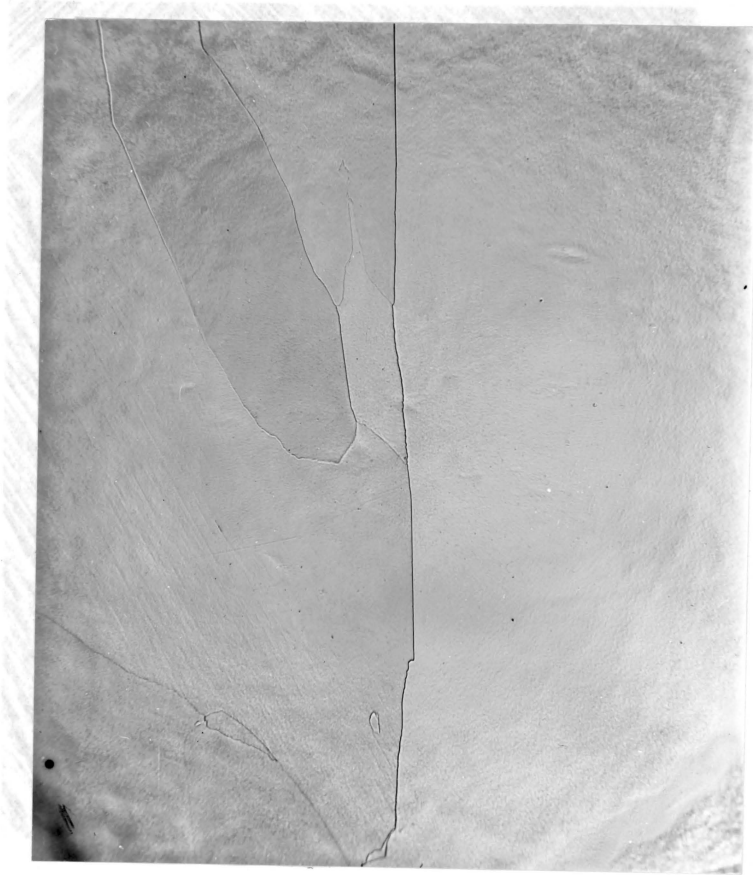


Figure 7. Typical As Melted Structure of Alloy Buttons,
Ti- 6.5 Weight Percent Aluminum. 50X
Aluminum, not forged in 100X field (2100 F). 100X

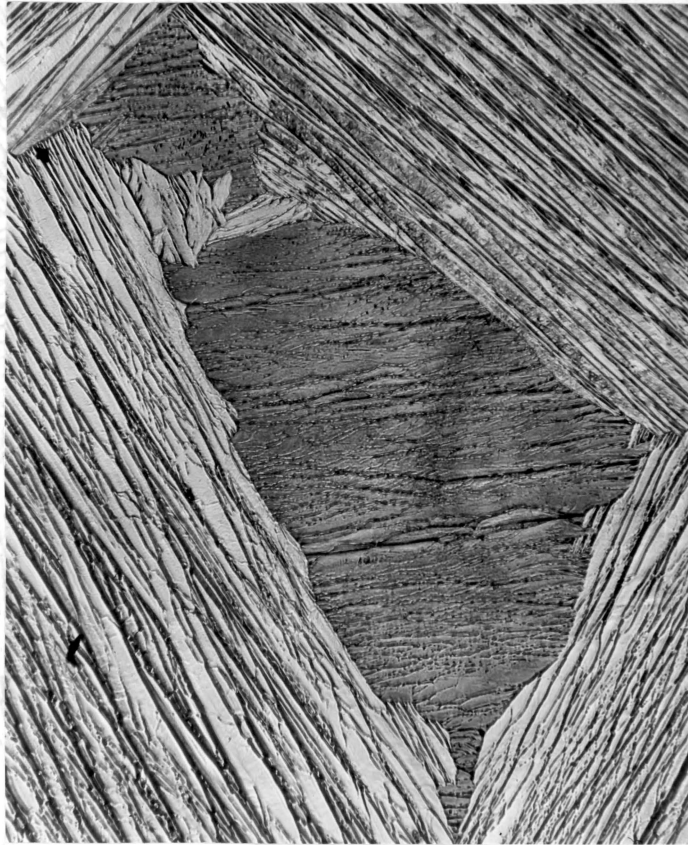
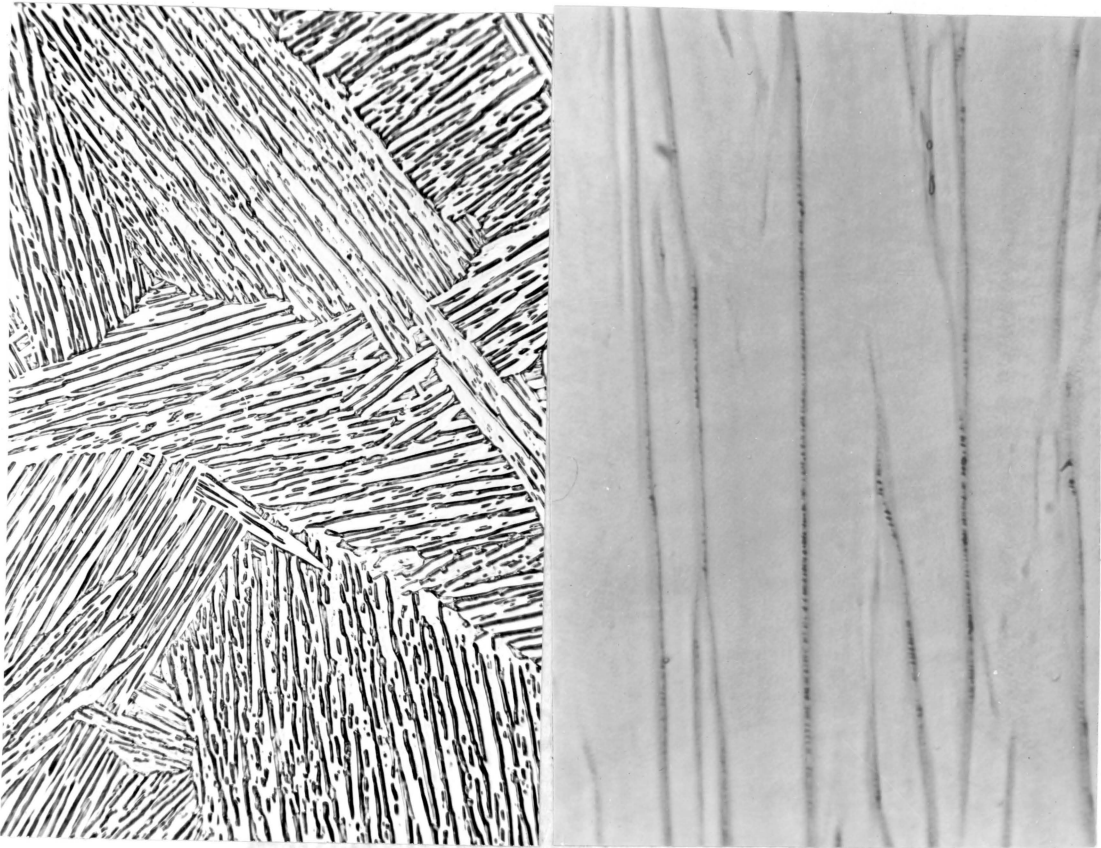


Figure 8. Typical Hot Forged Structure, Ti- 8 Weight Percent Aluminum, Hot Forged in Beta Field (2200°F). 100X



50X

1000X

Figure 9. Ti_3Al Visible in Widmanstätten Platelet Boundaries. Ti- 8 Weight Percent Aluminum, As received hot forged structure was Beta annealed for 24 hours at $2200^{\circ}F$, Specimen was then given a Ti_3Al precipitation anneal for 5 hours at $1100^{\circ}F$.



Figure 10. Ti_3Al Annealed Out of Platelet Boundaries.

Same specimen as Figure 9 except it has been given a further Alpha anneal at $1650^{\circ}F$ for 24 hours to remove Ti_3Al . Specimen was air cooled after Alpha anneal.

1000X

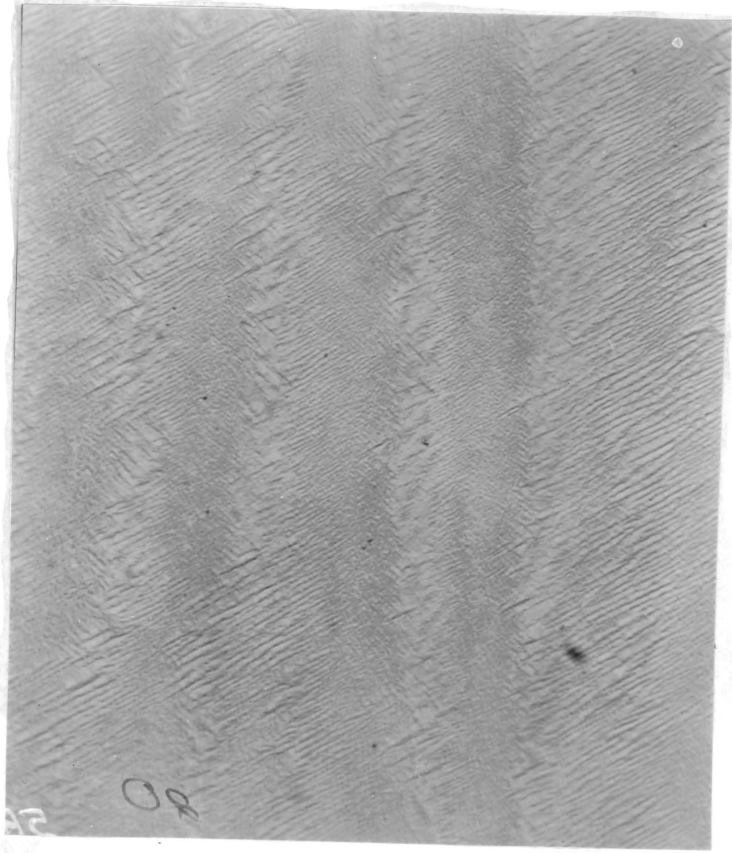
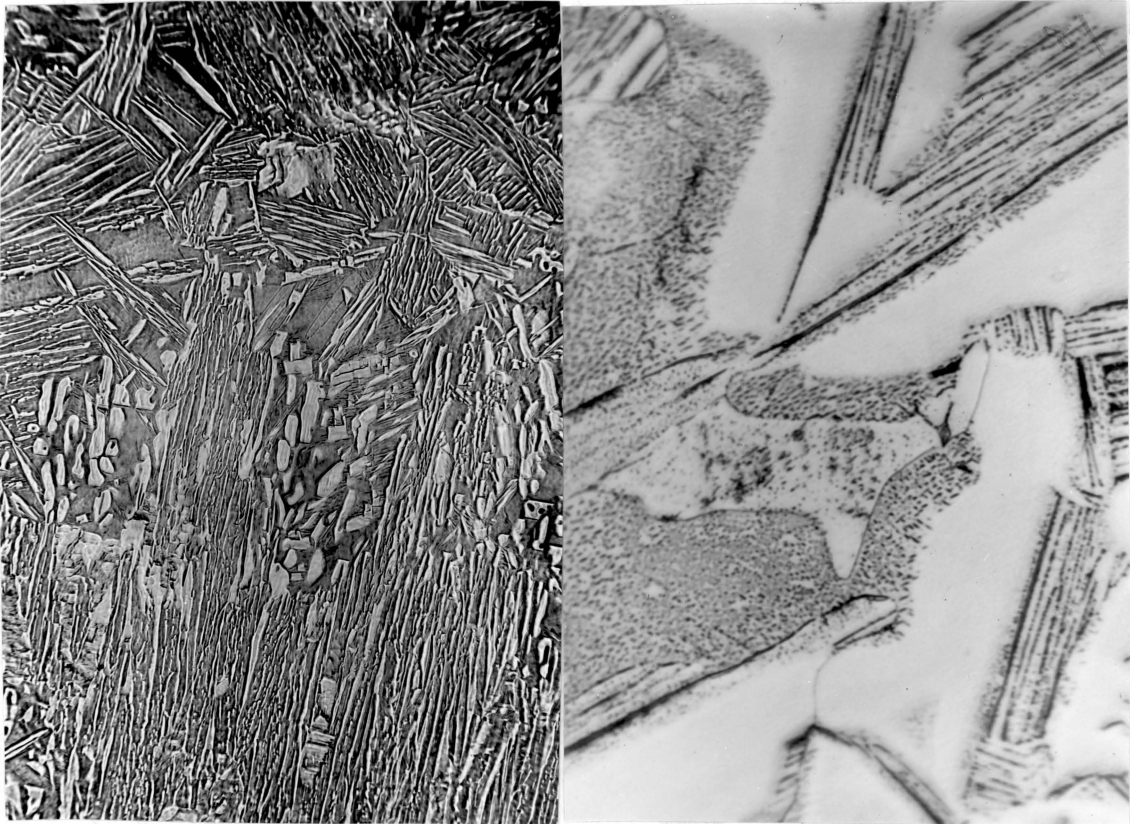


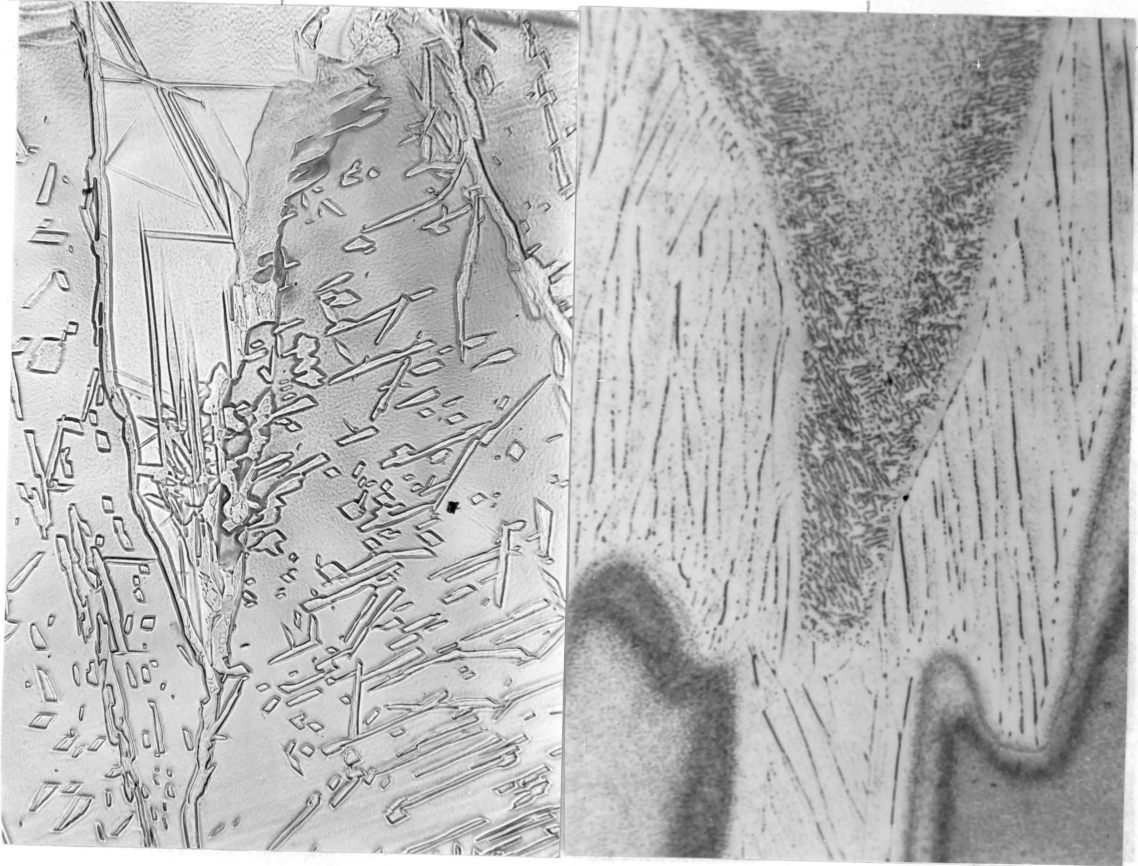
Figure 11. Martensitic Structure at Prior Platelate Boundaries. Same specimen as Figure 9 except it has been given a further Alpha anneal at 1650°F for 64 hours to remove Ti_3Al . Specimen was water quenched after Alpha anneal which resulted in martensitic structure at aluminum enriched platelate boundaries. 1000X



50X

1000X

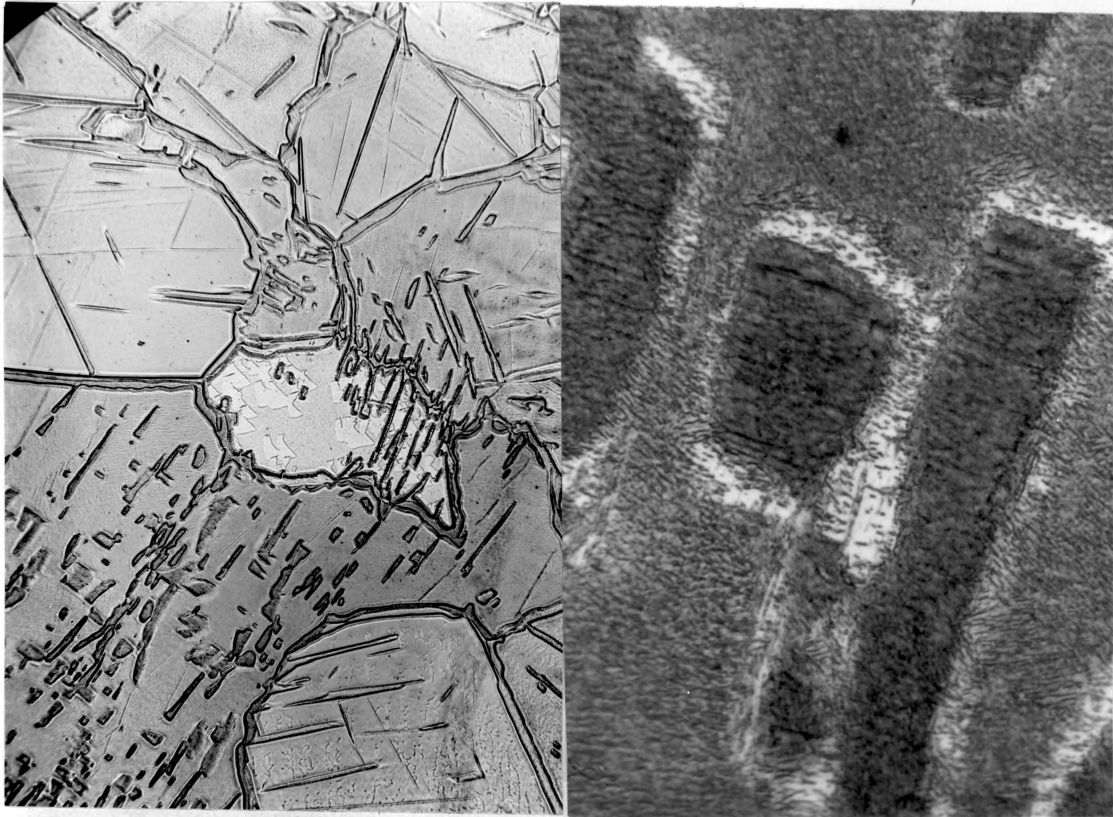
Figure 12. Segregation Anneal of Ti-4.1 Weight Percent Aluminum Alloy. As melted button was heat treated for 2 hours at 1780°F (970°C) and water quenched.



50X

1000X

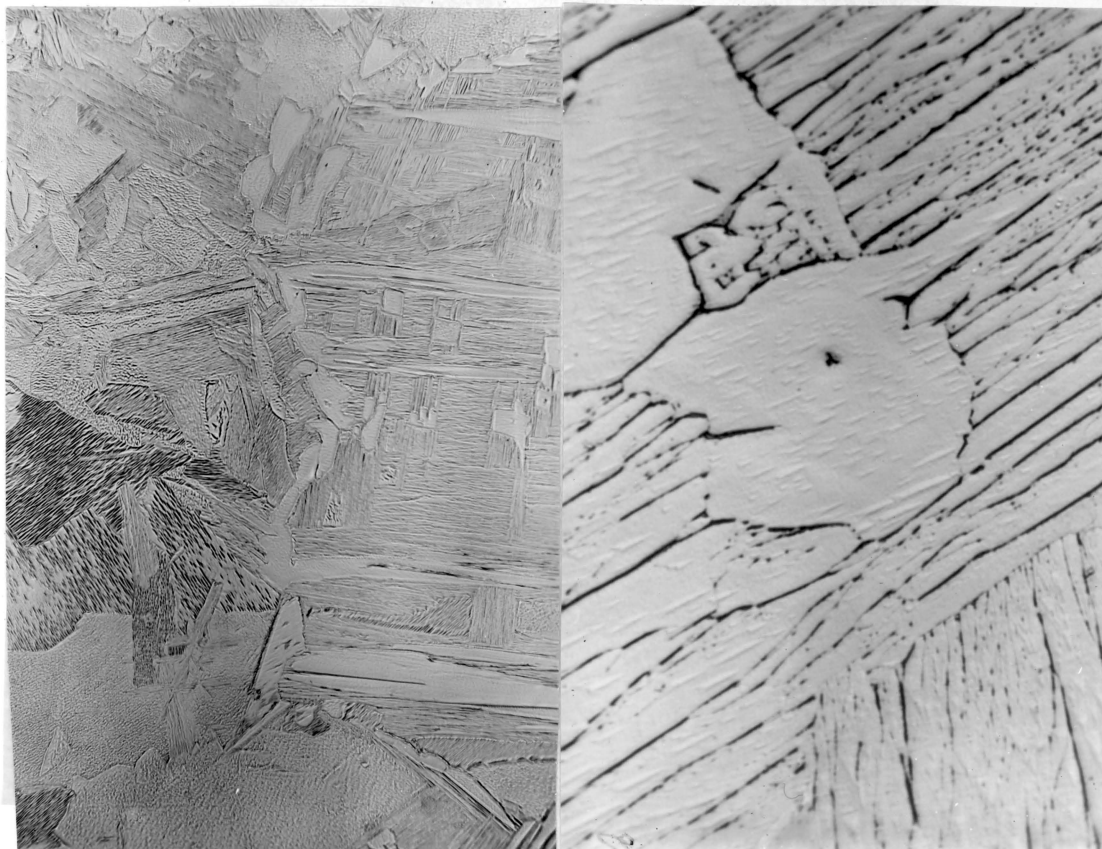
Figure 13. Segregation Anneal of 6.5 Weight Percent Aluminum Alloy. As melted button was heat treated for 8 hours at 1870°F (1020°C) and furnace cooled.



50X

1000X

Figure 14. Alpha Anneal of Ti-6.5 Weight Percent Aluminum Segregation Anneal. Same specimen as Figure 13 except it has been further annealed at 1650°F for 48 hours.



50X

1000X

Figure 15. Segregation Anneal of Ti- 9.0 Weight Percent Aluminum Alloy. As melted button was heat treated for 8 hours at 1960°F (1070°C) and water quenched.

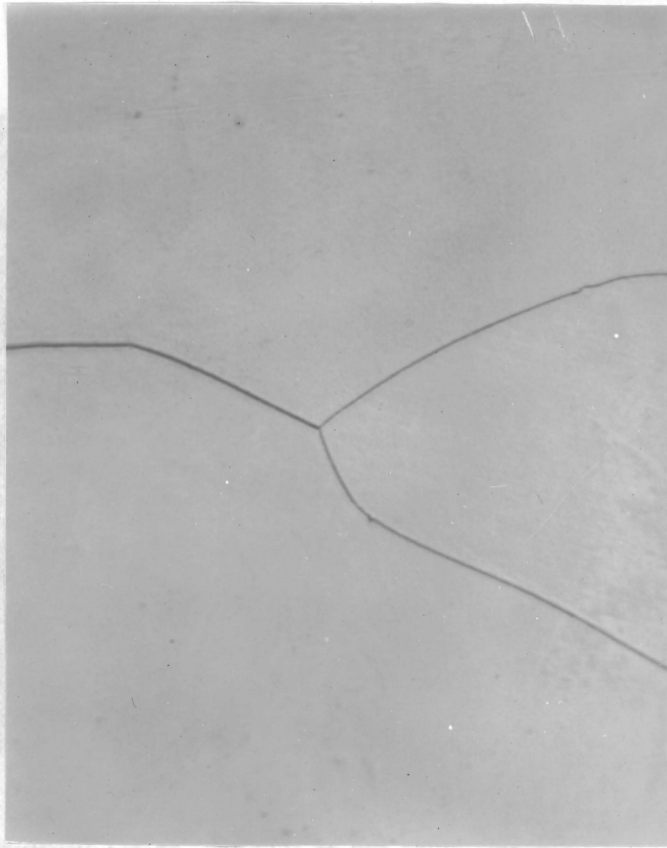
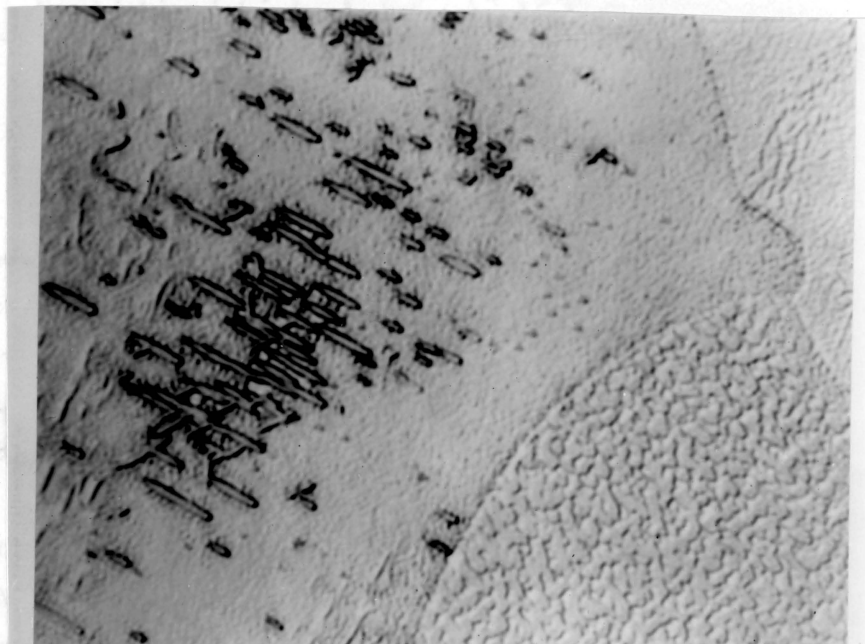


Figure 16. Alpha Anneal of Ti- 9.0 Weight Percent Aluminum Segregation Anneal. Same specimen as Figure 15 except it has been further annealed at 1850°F for 240 hours. 1000X



P 6084

X3000

Ti-7.1Al-0.05(O) (12 at. pct Al): α SHT 975°C (1790°F)-1 hr-WQ,
650°C (1200°F)-500 hr. Fully developed Ti_3Al precipitate in
 α matrix. Impact energy of 84 ft-lb at -80°F.

Figure 17. Overaged Ti_3Al Precipitate in Equiaxed Alpha Structure
Observed by Crossley⁽³⁴⁾.

FORMATION OF Ti_3Al AND ITS EMBRITTLING EFFECTS
ON TITANIUM-ALUMINUM ALLOYS

by

Frank Edward Brauer

Abstract

The formation of Ti_3Al and its embrittling characteristics have been investigated in Ti-Al binary alloys up to 9.0 weight percent aluminum. The investigating tools were optical metallography, the Brown-type stress corrosion test, and the Charpy V-notch Impact test. Segregated microstructures resulting from annealing in the $(\alpha + \beta)$ region were found to be extremely difficult to homogenize below the α -transus and could possibly explain the two phase regions reported by many investigators. Sea-water stress corrosion tests reveal that a Widmanstätten structure is susceptible to stress corrosion cracking after aging for two hours at $1100^\circ F$. Much longer annealing times are required to produce susceptibility in equiaxed α -grains resulting from annealing in the $(\alpha + \beta)$ region. Toughness is less affected as a result of aging a Widmanstätten structure than an equiaxed structure, although the reduction is significant in both cases.